Causes and Implications of Persistent Atmospheric Carbon Dioxide Biases in Earth System Models

Forrest M. Hoffman, James T. Randerson, Vivek K. Arora, Qing Bao, Katharina D. Six, Patricia Cadule, Duoying Ji, Chris D. Jones, Michio Kawamiya, Samar Khatiwala, Keith Lindsay, Atsushi Obata, Elena Shevliakova, Jerry F. Tjiputra, Evgeny M. Volodin, Tongwen Wu

2013 AGU Fall Meeting
Presentation B13M-07

December 9, 2013

U.S. DEPARTMENT OF ENERGY

UCI DEPARTMENT OF EARTH SYSTEM SCIENCE

UCIRVINE

Climate Change Science Institute
AT OAK RIDGE NATIONAL LABORATORY

OAK RIDGE NATIONAL LABORATORY
MANAGED BY UT-BATTELLE FOR THE U.S. DEPARTMENT OF ENERGY

Research Questions

Question 1

How well do Earth System Models (ESMs) simulate the observed distribution of anthropogenic carbon in atmosphere, ocean, and land reservoirs?

Research Questions

Question 1

How well do Earth System Models (ESMs) simulate the observed distribution of anthropogenic carbon in atmosphere, ocean, and land reservoirs?

Question 2

Can we use contemporary atmospheric CO_2 observations to constrain future CO_2 projections?

Observed Carbon Accumulation Since 1850

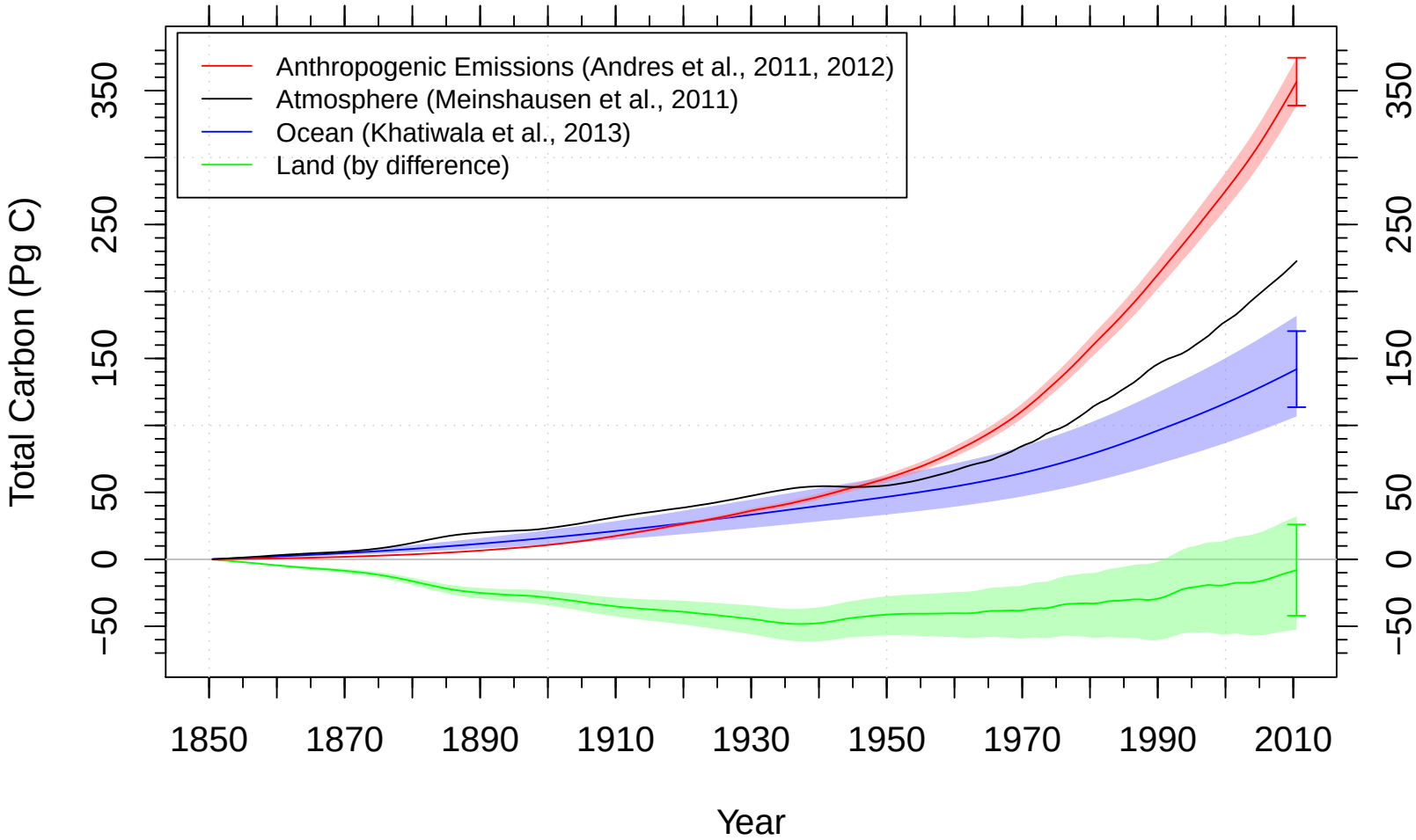

Observational estimates of anthropogenic carbon emissions (excluding land use change) and accumulation in atmosphere, ocean, and land reservoirs for 1850–2010. Atmosphere carbon is a fusion of Law Dome ice core CO_2 observations, the Keeling Mauna Loa record, and more recently the NOAA GMD global surface average, integrated for the purpose of forcing IPCC models. Total land flux is computed by mass balance as follows:

$$\Delta C_L = \sum_i F_i - \Delta C_A - \Delta C_O.$$

15 fully-prognostic ESMs that performed CMIP5 emissions-forced simulations

Model	Modeling Center
BCC-CSM1.1	Beijing Climate Center, China Meteorological Administration, CHINA
BCC-CSM1.1(m)	Beijing Climate Center, China Meteorological Administration, CHINA
BNU-ESM	Beijing Normal University, CHINA
CanESM2	Canadian Centre for Climate Modelling and Analysis, CANADA
CESM1-BGC	Community Earth System Model Contributors, NSF-DOE-NCAR, USA
FGOALS-s2.0	LASG, Institute of Atmospheric Physics, CAS, CHINA
GFDL-ESM2g	NOAA Geophysical Fluid Dynamics Laboratory, USA
GFDL-ESM2m	NOAA Geophysical Fluid Dynamics Laboratory, USA
HadGEM2-ES	Met Office Hadley Centre, UNITED KINGDOM
INM-CM4	Institute for Numerical Mathematics, RUSSIA
IPSL-CM5A-LR	Institut Pierre-Simon Laplace, FRANCE
MIROC-ESM	Japan Agency for Marine-Earth Science and Technology, Atmosphere and Ocean Research Institute (University of Tokyo), and National Institute for Environmental Studies, JAPAN
MPI-ESM-LR	Max Planck Institute for Meteorology, GERMANY
MRI-ESM1	Meteorological Research Institute, JAPAN
NorESM1-ME	Norwegian Climate Centre, NORWAY

CMIP5 Long-Term Experiments

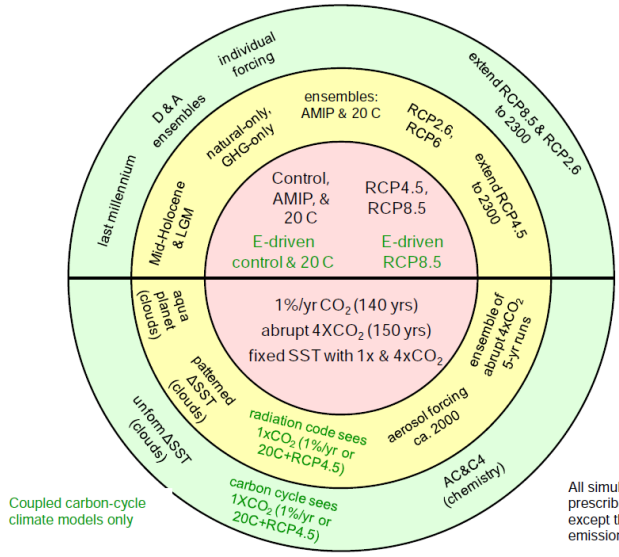

Emissions for Historical + RCP 8.5 Simulations

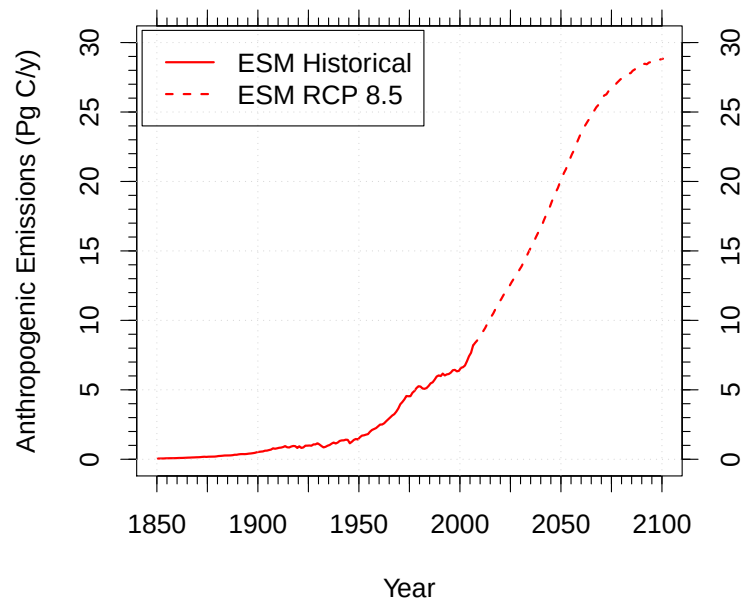

(a) Most ESMs exhibit a high bias in predicted atmospheric CO_2 mole fraction, which ranges from 357–405 ppm at the end of the historical period (1850–2005).

(b) The multi-model mean is biased high from 1946 throughout the 20th century, ending 5.6 ppm above the observed value of 378.8 ppm in 2005.

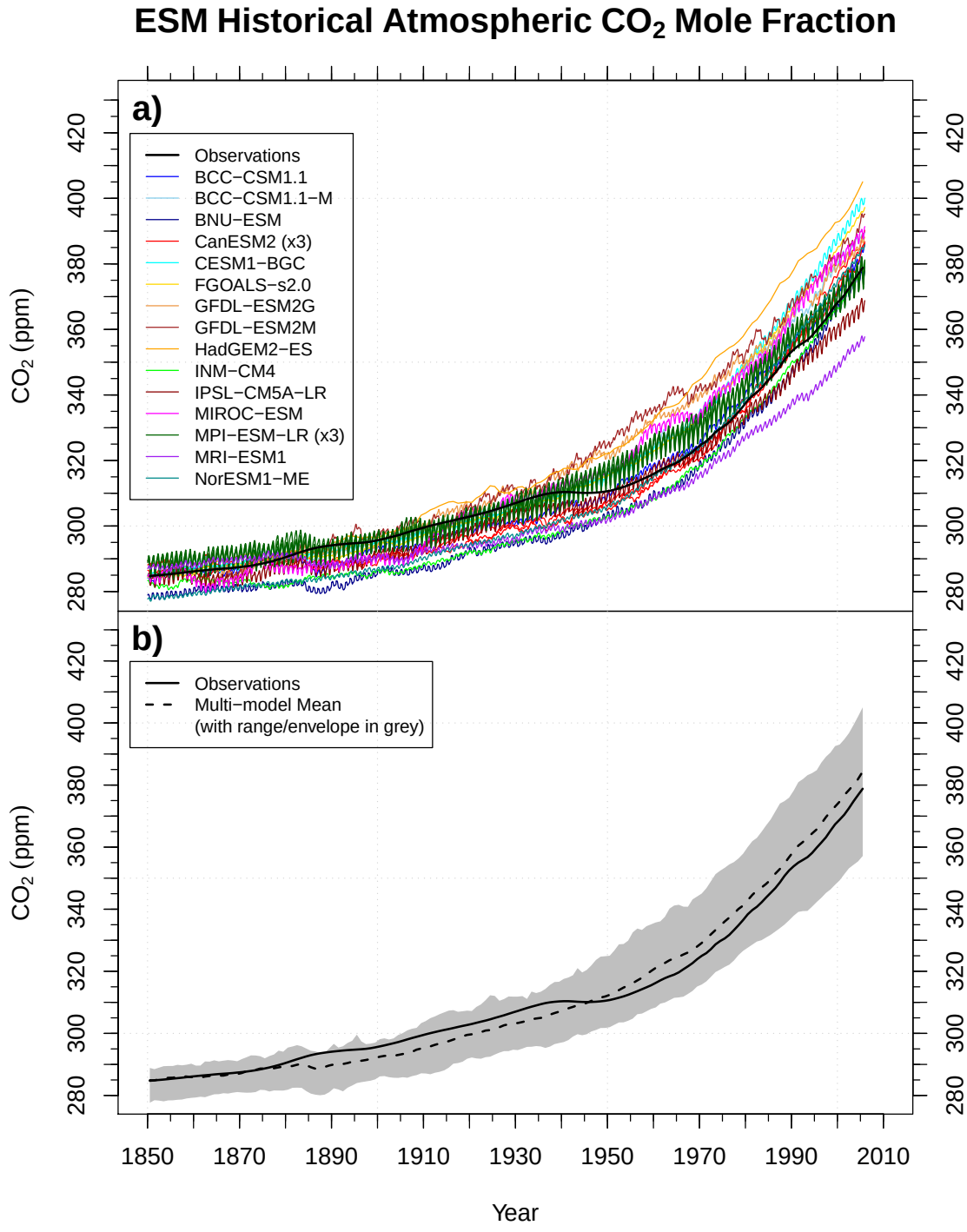

Model inventory comparison with Khatiwala et al. (2013)

Once normalized by their atmospheric carbon inventories, most ESMs exhibit a low bias in anthropogenic ocean carbon accumulation through 2010.

The same pattern holds for the Sabine et al. (2004) inventory derived using the ΔC^* separation technique.

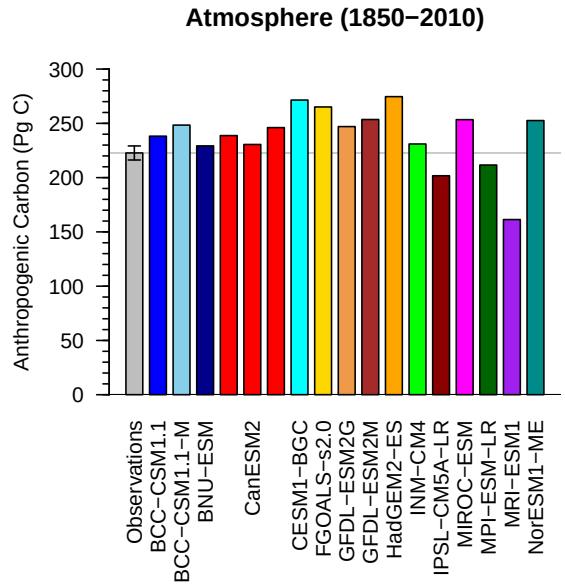

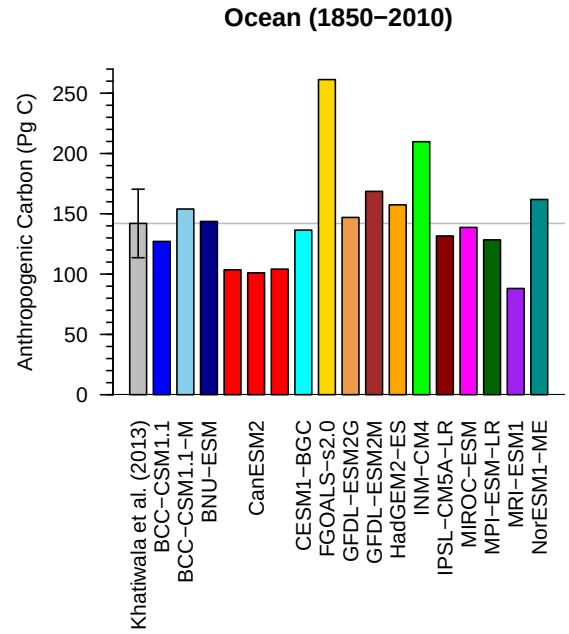

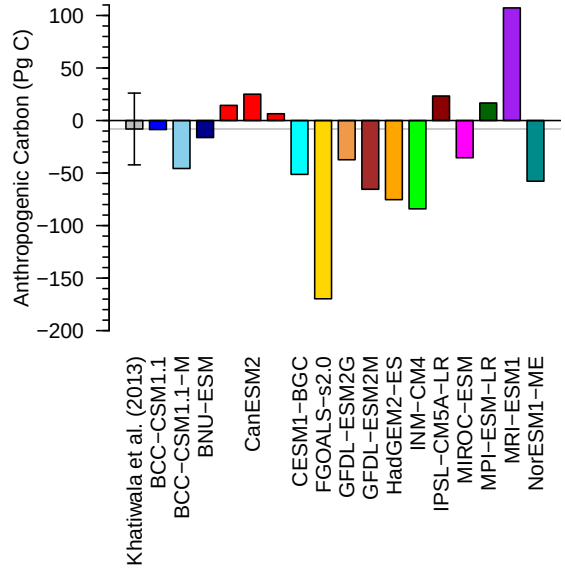

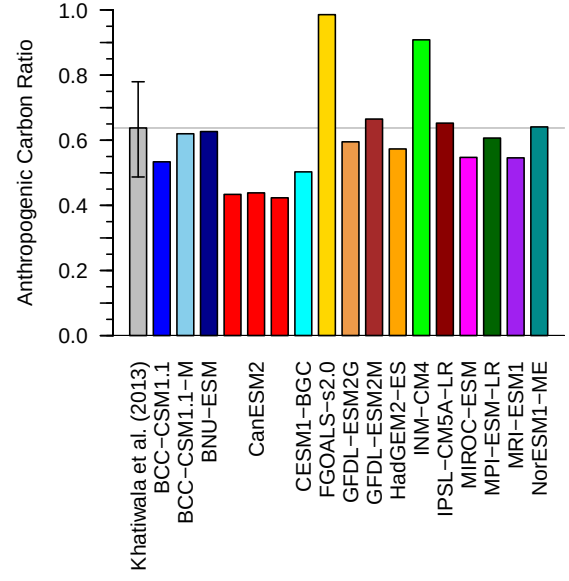

(a) Ocean inventory estimates have a fairly persistent ordering during the second half of the 20th century.

(b) ESMs have a wide range of land carbon accumulation responses to increasing CO_2 and land use change, ranging from a net source of 170 Pg C to a sink of 107 Pg C in 2010.

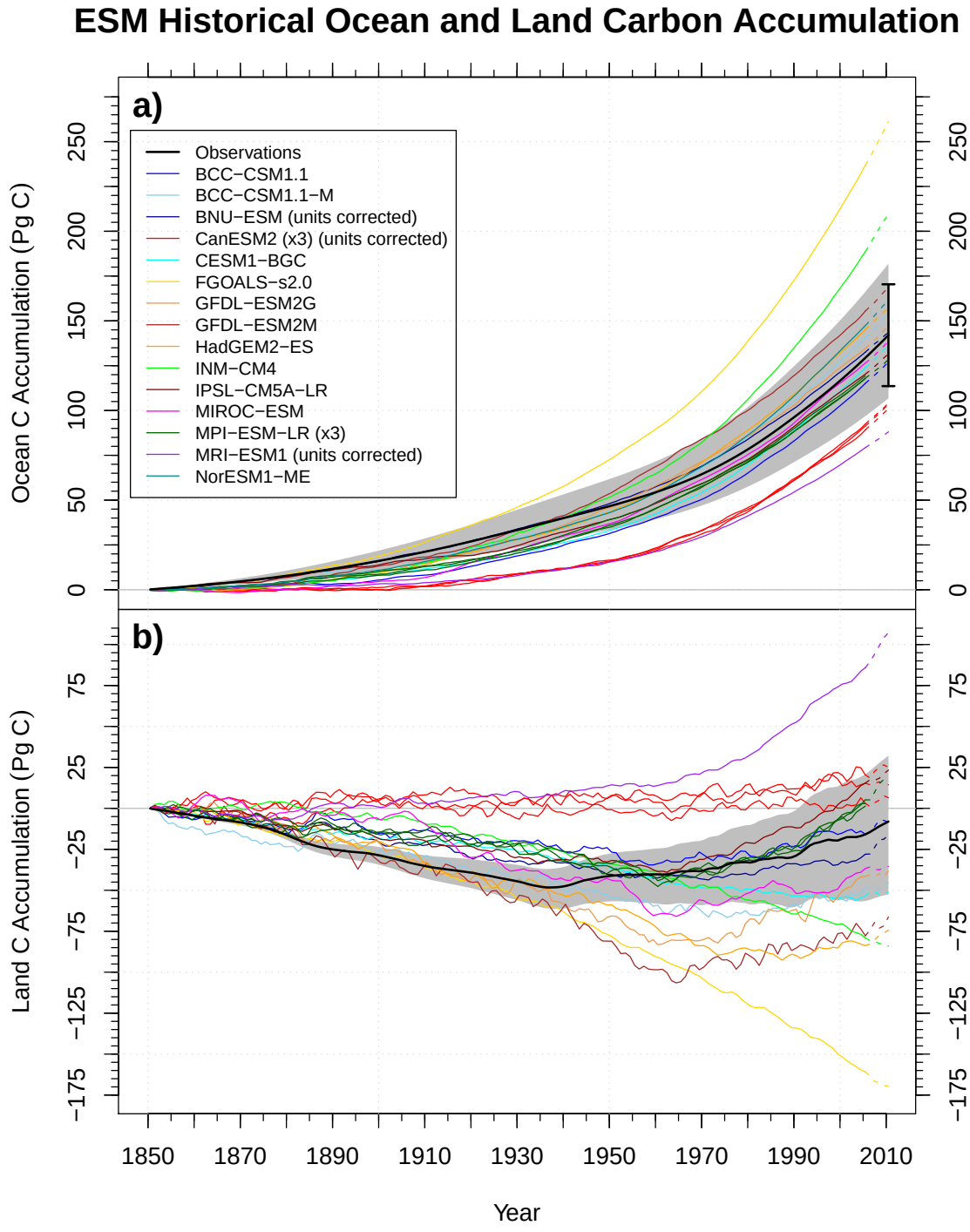

Question 1

How well do Earth System Models (ESMs) simulate the observed distribution of anthropogenic carbon in atmosphere, ocean, and land reservoirs?

- Most ESMs exhibit a high bias in predicted atmospheric CO_2 mole fraction, ranging from 357–405 ppm in 2005.
- The multi-model mean atmospheric CO_2 mole fraction is biased high from 1946 onward, ending 5.6 ppm above observations in 2005.
- Once normalized by atmospheric carbon accumulation, most ESMs exhibit a low bias in ocean accumulation in 2010.
- ESMs predict a wide range of land carbon accumulation in response to increasing CO_2 and land use change, ranging from -170–107 Pg C in 2010.

Question 2

Can we use contemporary atmospheric CO_2 observations to constrain future CO_2 projections?

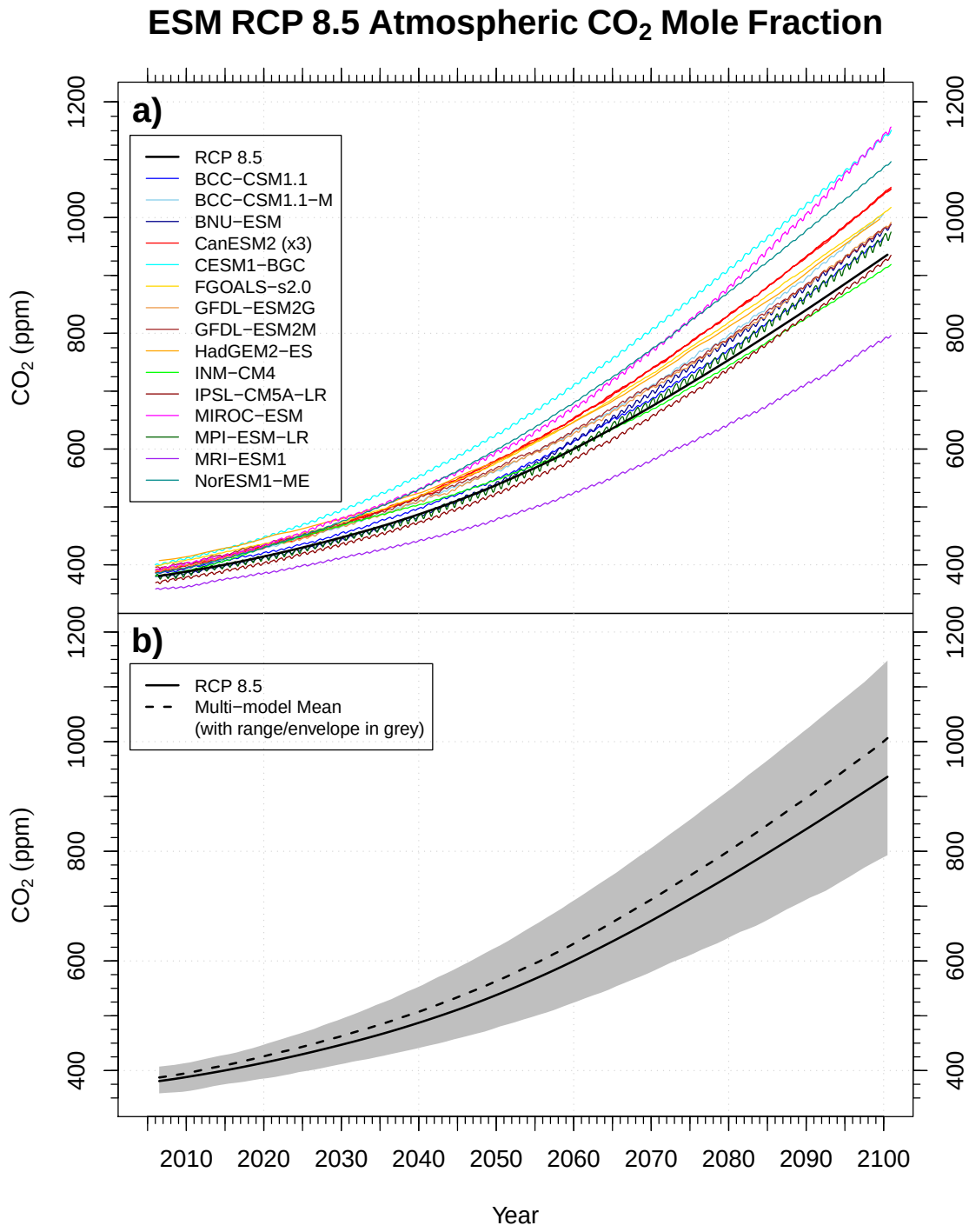

Reducing Uncertainties Using Observations

To reduce feedback uncertainties using contemporary observations,

1. there must be a relationship between contemporary variability and future trends on longer time scales within the model, and

Reducing Uncertainties Using Observations

To reduce feedback uncertainties using contemporary observations,

1. there must be a relationship between contemporary variability and future trends on longer time scales within the model, and
2. it must be possible to constrain contemporary variability in the model using observations.

Reducing Uncertainties Using Observations

To reduce feedback uncertainties using contemporary observations,

1. there must be a relationship between contemporary variability and future trends on longer time scales within the model, and
2. it must be possible to constrain contemporary variability in the model using observations.

Example #1

Hall and Qu (2006) evaluated the strength of the springtime snow albedo feedback (SAF; $\Delta\alpha_s/\Delta T_s$) from 17 models used for the IPCC AR4 and compared them with the observed springtime SAF from ISCCP and ERA-40 reanalysis.

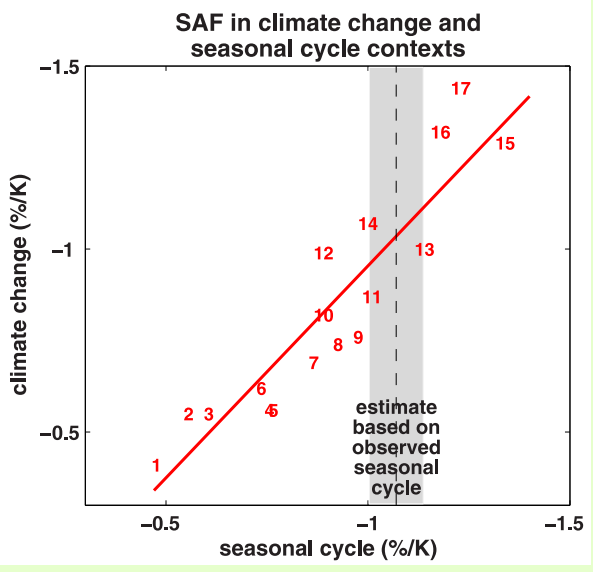

Reducing Uncertainties Using Observations

To reduce feedback uncertainties using contemporary observations,

1. there must be a relationship between contemporary variability and future trends on longer time scales within the model, and
2. it must be possible to constrain contemporary variability in the model using observations.

Example #2

Cox et al. (2013) used the observed relationship between the CO_2 growth rate and tropical temperature as a constraint to reduce uncertainty in the land carbon storage sensitivity to climate change (γ_L) in the tropics using C^4MIP models.

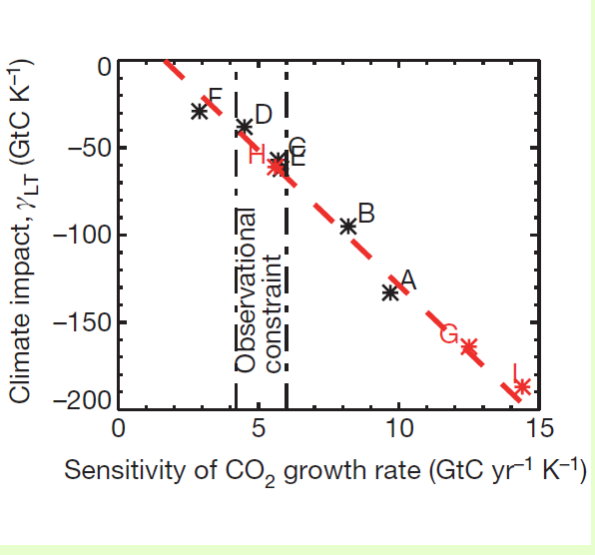

We developed a new emergent constraint from carbon inventories.

A relationship exists between contemporary and future atmospheric CO_2 levels over decadal time scales because carbon model biases persist over decadal time scales.

Observed contemporary atmospheric CO_2 mole fraction is represented by the vertical line at 384.6 ± 0.5 ppm.

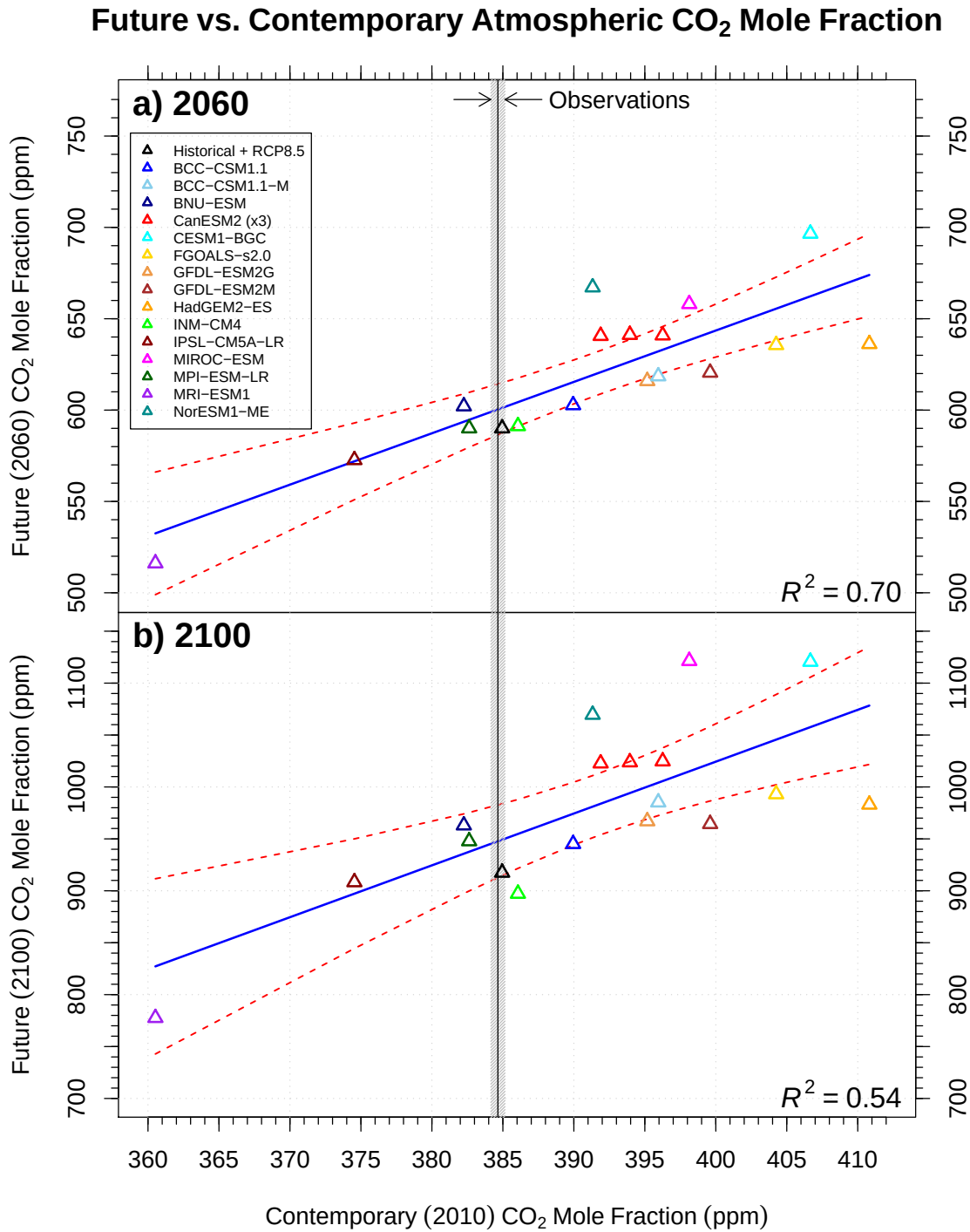

Removing pre-industrial CO_2 mole fraction biases from models, we found the relationship held, confirming the robustness of our result.

Observed contemporary anthropogenic atmospheric carbon inventory is represented by the vertical line at 213.4 ± 6.5 Pg C, which incorporates 1850 CO_2 mole fraction uncertainties.

Adding uncertainties from fossil fuel emissions increased uncertainty to ± 12.7 Pg C.

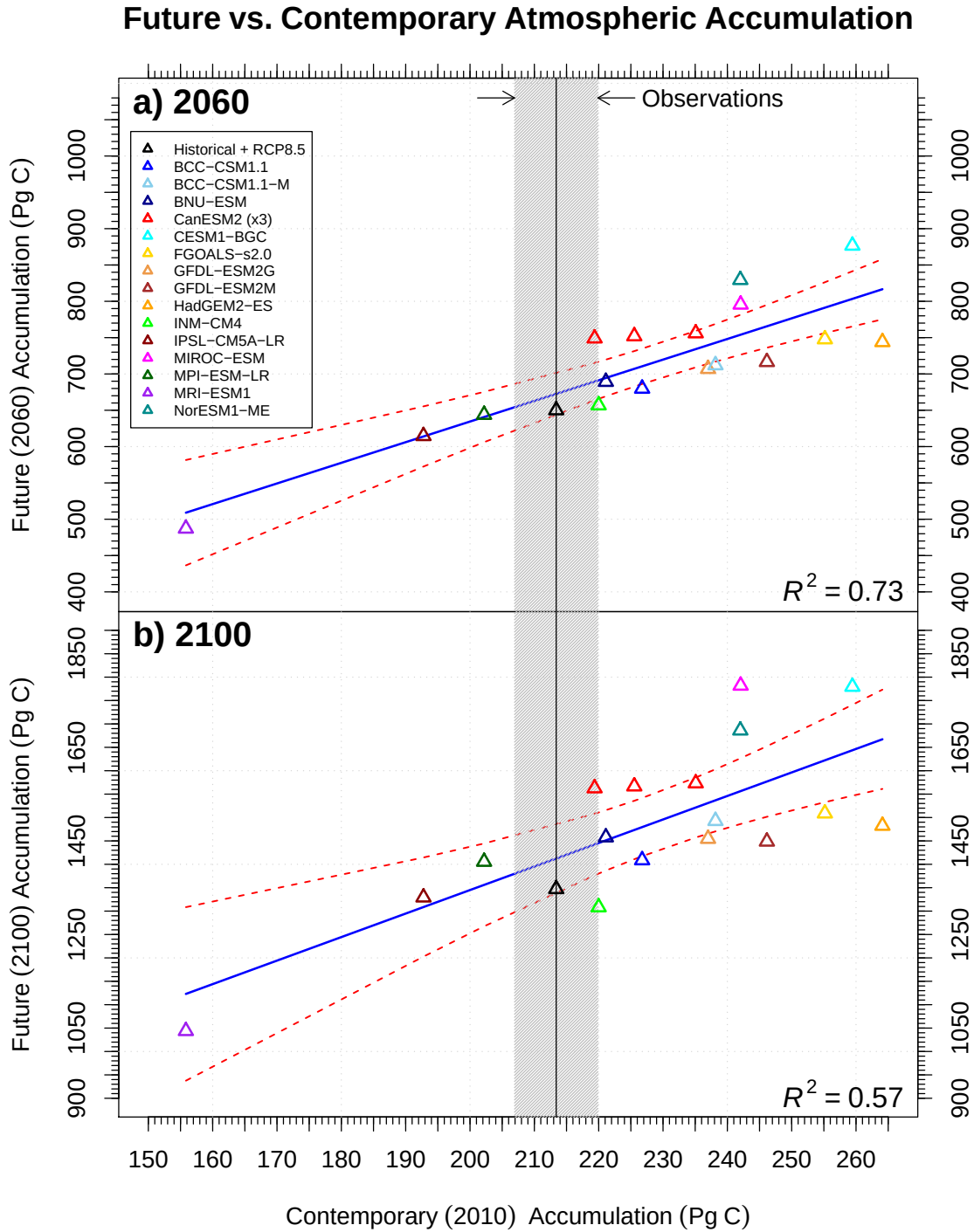

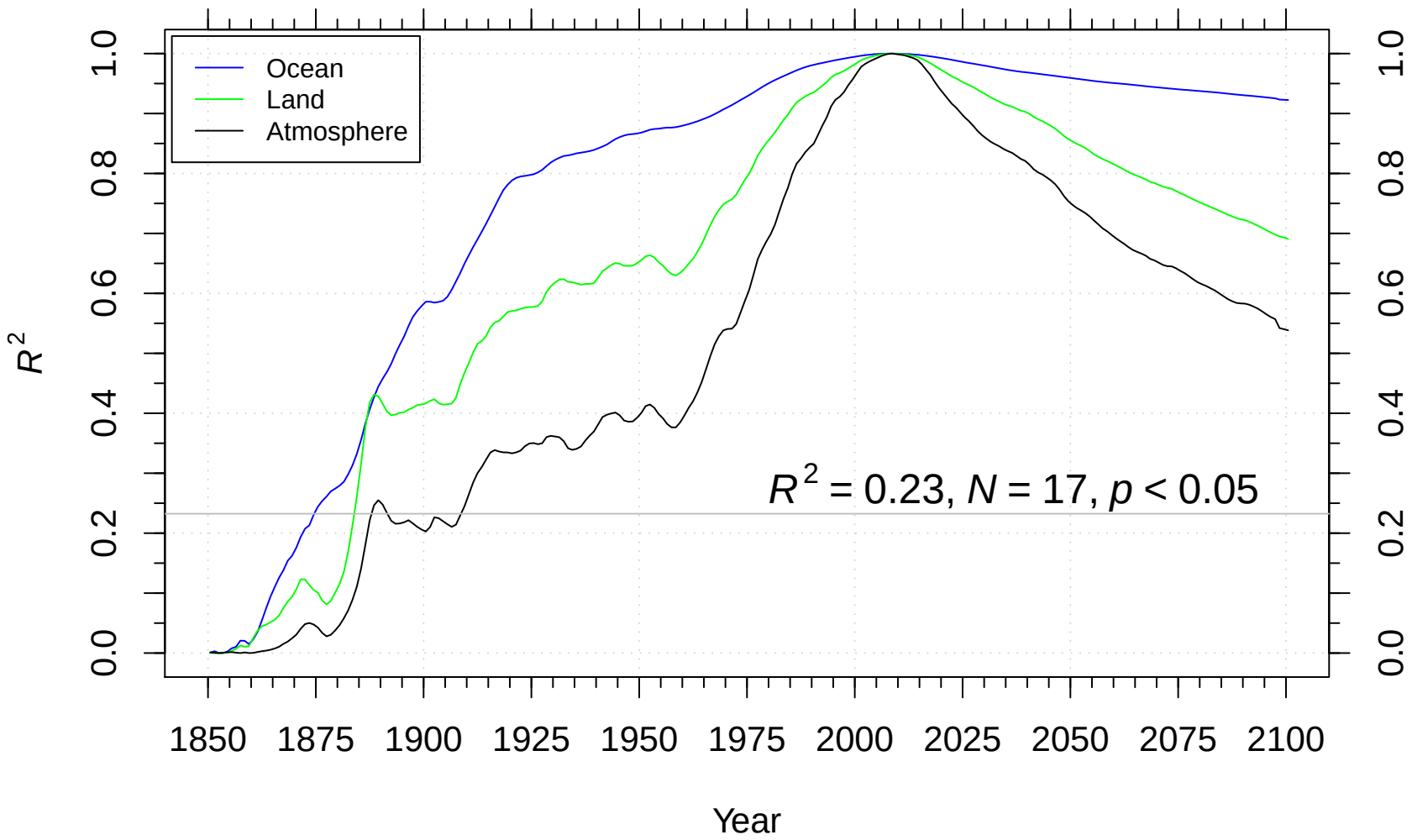

The coefficients of determination (R^2) for the multi-model bias structure relative to the set of CMIP5 model atmospheric CO_2 mole fractions (black), and oceanic (blue) and land (green) anthropogenic carbon inventories in 2010. Atmospheric CO_2 mole fractions are statistically significant for 1910–2100.

Contemporary CO_2 Tuned Model (CCTM)

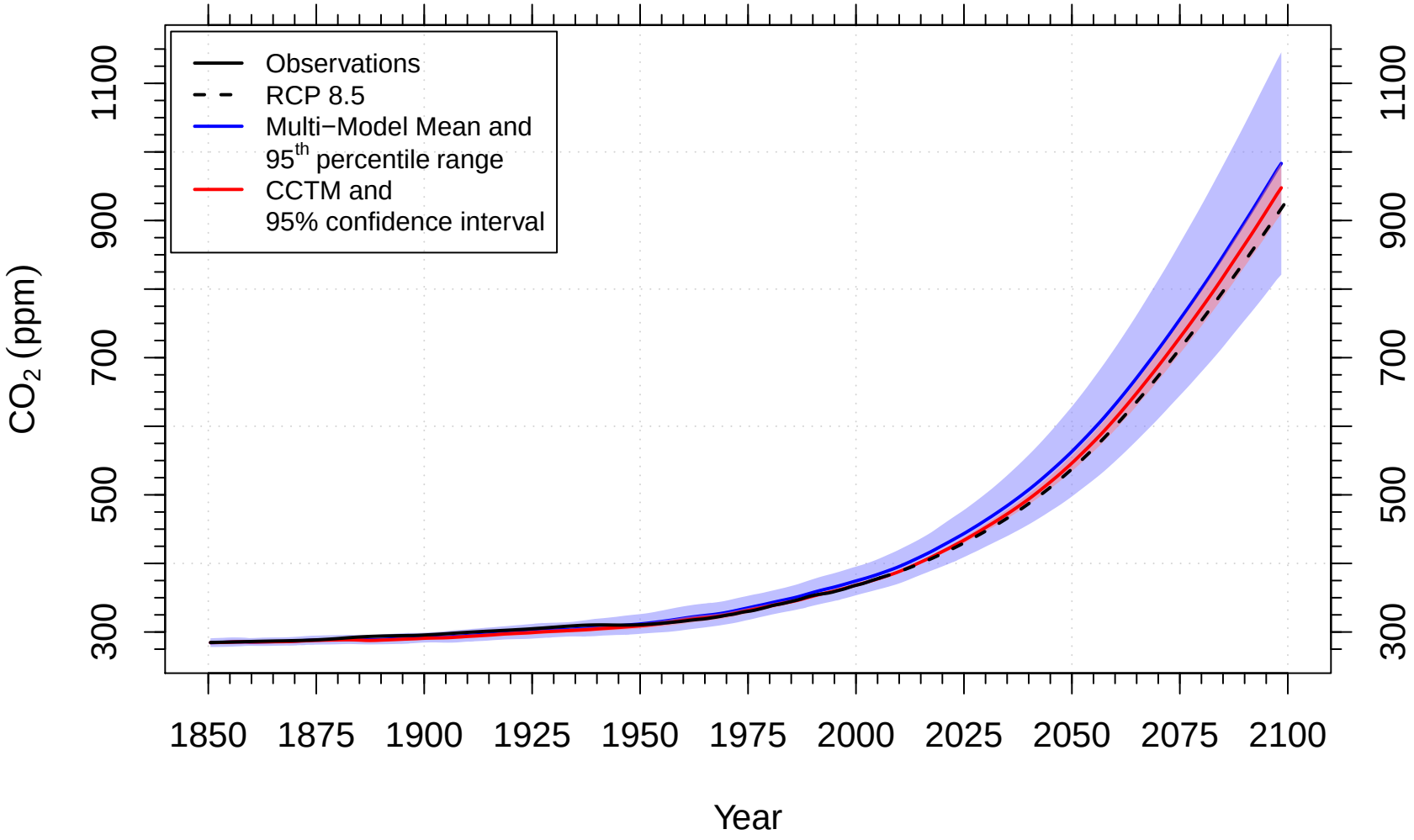

We used this regression to create a contemporary CO_2 tuned model (CCTM) estimate of the atmospheric CO_2 trajectory for the 21st century.

Best estimate developed using Mauna Loa CO_2 data:

At 2060: 600 ± 14 ppm, 21 ppm below the multi-model mean

At 2100: 947 ± 35 ppm, 32 ppm below the multi-model mean

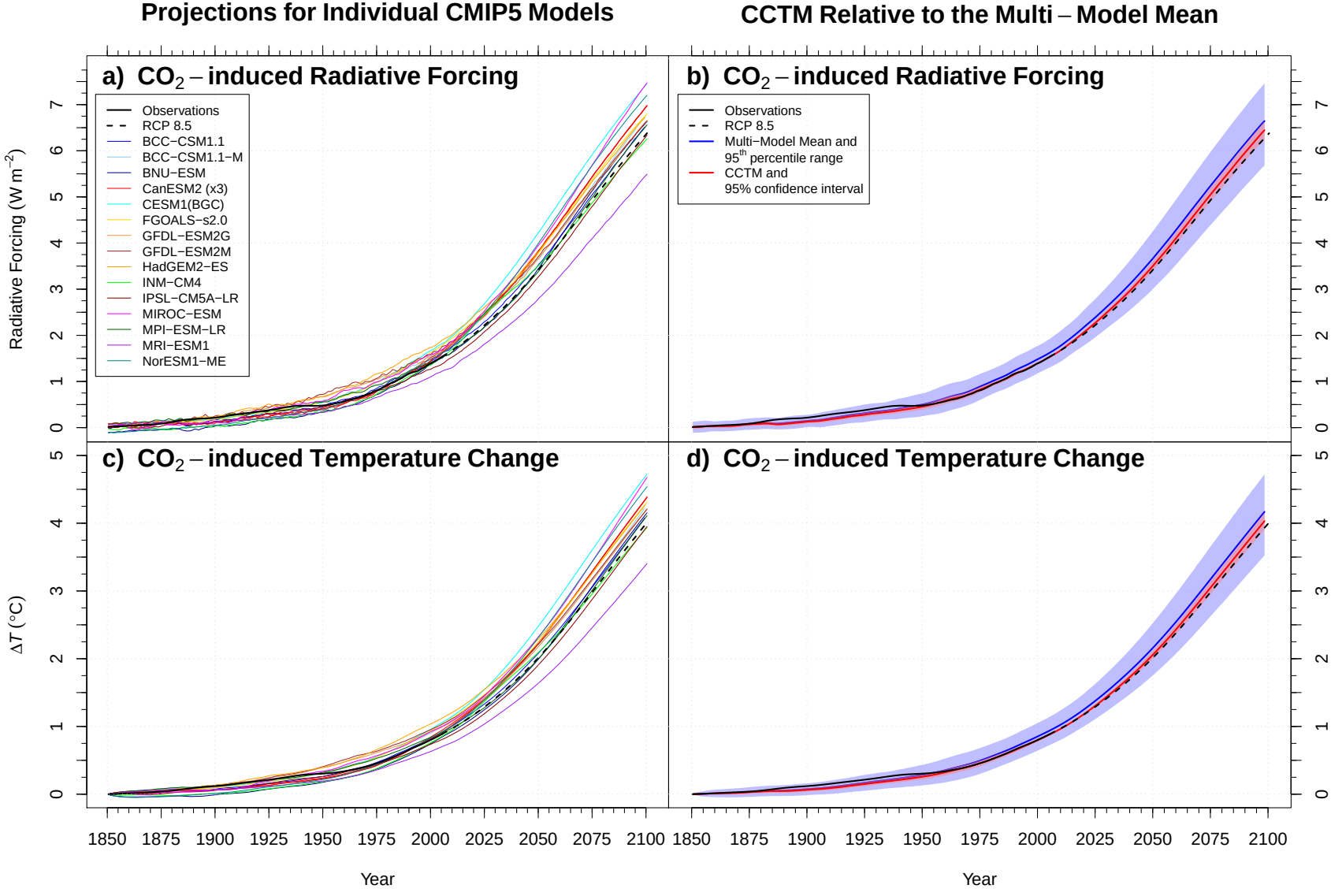

We calculated the CO_2 radiative forcing and used an impulse response function (tuned to the mean transient climate response of CMIP5 models) to equitably compute the resulting CO_2-induced temperature change (ΔT_{CO_2}) for models and the CCTM. The CO_2 biases for individual models contributed to ΔT_{CO_2} biases of -0.7°C to $+0.6^{\circ}$C by 2100, relative to the CCTM estimate.

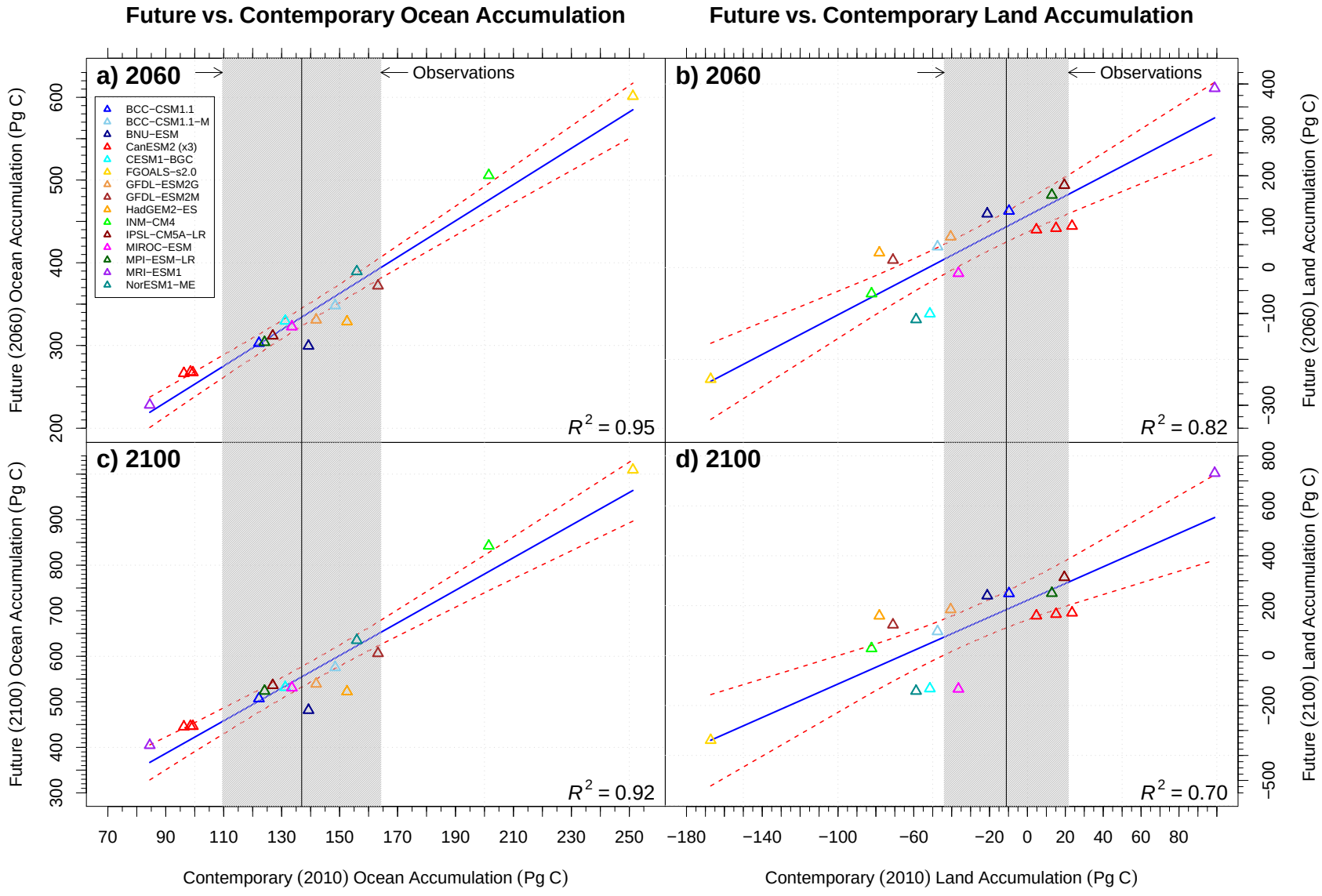

We also developed a multi-model constraint on the evolution of ocean and land anthropogenic inventories. Since observational uncertainties are higher for ocean and land, uncertainties in future estimates cannot be reduced as much as for atmospheric CO_2.

Question 2

Can we use contemporary CO_2 observations to constrain future CO_2 projections?

- Yes.

Question 2

Can we use contemporary CO_2 observations to constrain future CO_2 projections?

- Yes.
- We developed a new emergent constraint from anthropogenic carbon inventories in atmosphere, ocean, and land reservoirs.
- Land and ocean processes contributing to contemporary carbon cycle biases persist over decadal timescales.
- We used the relationship between contemporary and future atmospheric CO_2 levels to create a contemporary CO_2 tuned model (CCTM) estimate for the 21^{st} century.
  - At 2060: 600 ± 14 ppm, 21 ppm below the multi-model mean.
  - At 2100: 947 ± 35 ppm, 32 ppm below the multi-model mean.
- Uncertainties in future climate predictions may be reduced by improving models to match the long-term time series of CO_2 from Mauna Loa and other monitoring stations.

Conclusions

- A considerable amount of the model-to-model variability of CO_2 in the 21st century can be traced to biases that exist at the end of the observational record.
- Bias persistence was highest for the ocean, followed by land, and then by the atmosphere.
- Carbon cycle biases are likely primarily linked with concentration–carbon feedback processes:
  - ocean – Southern Ocean overturning, vertical mixing processes
  - land – CO_2 fertilization, allocation to woody pools, nutrient limitation
- Future fossil fuel emissions targets designed to stabilize CO_2 levels would be too low if estimated from the multi-model mean of ESMs.
  - ESMs overestimate contemporary CO_2 with observed emissions.
- Models could be improved through extensive comparison with observations and community model benchmarking.

Acknowledgments

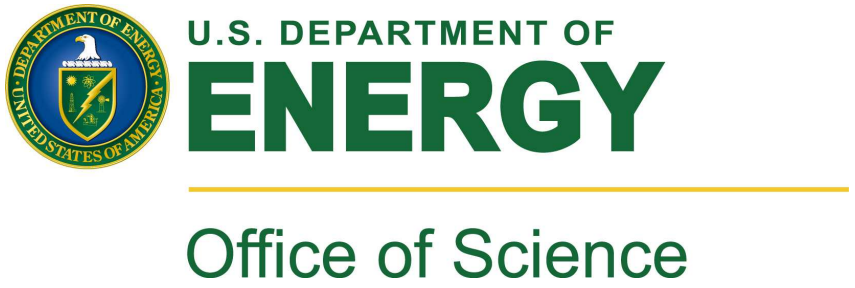

This research was sponsored by the Climate and Environmental Sciences Division (CESD) of the Biological and Environmental Research (BER) Program in the U. S. Department of Energy Office of Science and the National Science Foundation (AGS-1048890). This research used resources of the National Center for Computational Sciences (NCCS) at Oak Ridge National Laboratory (ORNL), which is managed by UT-Battelle, LLC, for the U. S. Department of Energy under Contract No. DE-AC05-00OR22725. CDJ was supported by the Joint DECC/Defra Met Office Hadley Centre Climate Programme (GA01101). This is a contribution to the BIOFEEDBACK project of the Center for Climate Dynamics (SKD) at the Bjerknes Centre for Climate Research. The National Center for Atmospheric Research is sponsored by the National Science Foundation.

We acknowledge the World Climate Research Programme's Working Group on Coupled Modelling, which is responsible for CMIP, and we thank the climate modeling groups for producing and making available their model output. For CMIP the U. S. Department of Energy's Program for Climate Model Diagnosis and Intercomparison provides coordinating support and led development of software infrastructure in partnership with the Global Organization for Earth System Science Portals.

Extra Slides

Model inventory comparison with Sabine et al. (2004)

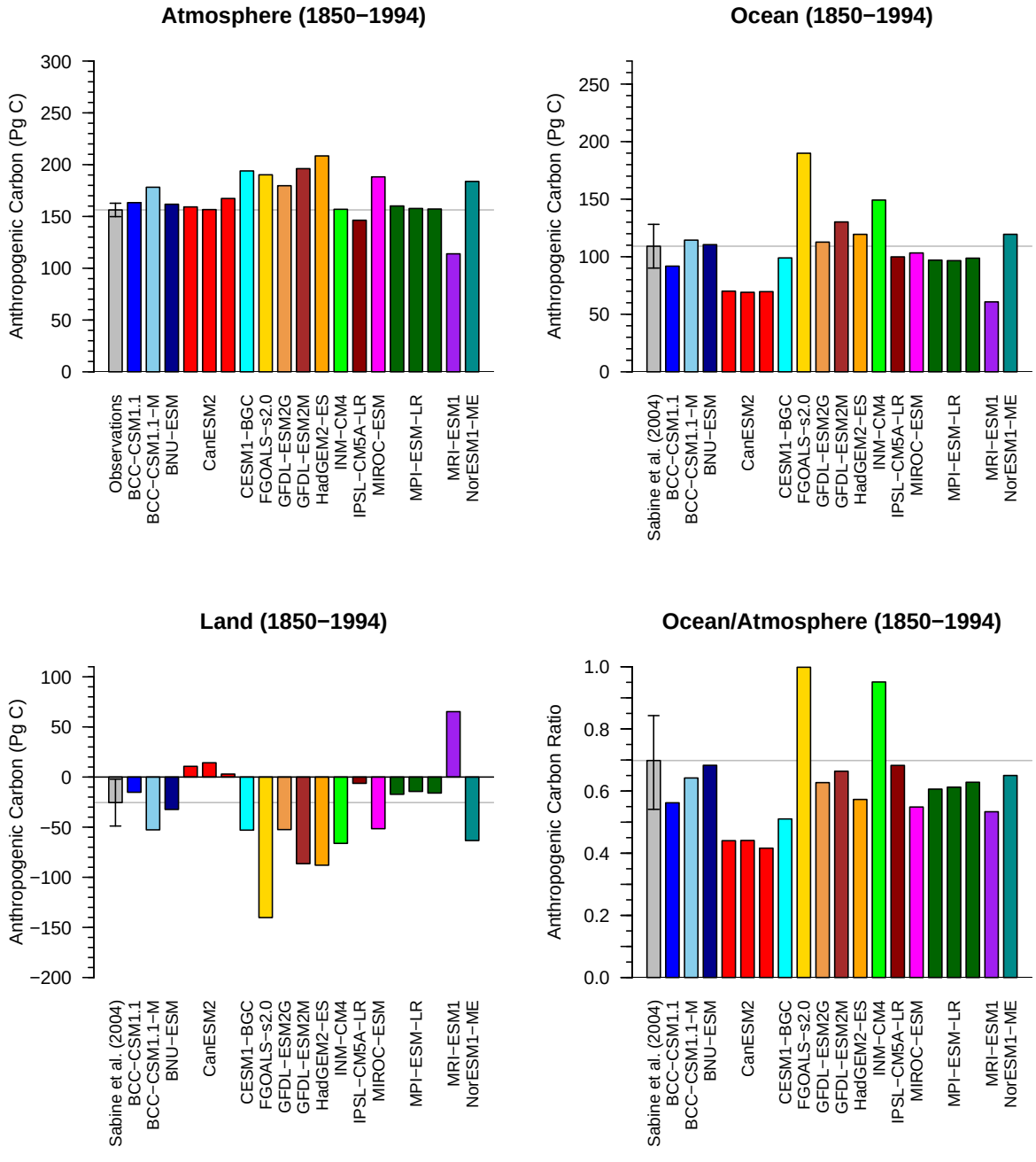

Implications for CO_2, Radiative Forcing, and Temperature

Model	CO_2 Mole Fraction (ppm)			Radiative Forcing ($W\,m^{-2}$)			Cumulative ΔT (°C)			ΔT Bias (°C)		
	2010	2060	2100	2010	2060	2100	2010	2060	2100	2010	2060	2100
BCC-CSM1.1	390	603	945	1.70	4.03	6.43	0.97	2.39	4.02	0.03	0.02	−0.01
BCC-CSM1.1-M	396	619	985	1.78	4.16	6.65	1.04	2.49	4.16	0.10	0.12	0.13
BNU-ESM	382	602	963	1.59	4.02	6.53	0.90	2.33	4.07	−0.04	−0.04	0.04
CanESM2 r1	394	641	1024	1.75	4.36	6.86	0.98	2.58	4.30	0.04	0.21	0.27
CanESM2 r2	392	641	1023	1.72	4.35	6.85	0.98	2.57	4.30	0.04	0.20	0.27
CanESM2 r3	396	641	1025	1.78	4.35	6.87	1.01	2.58	4.30	0.07	0.21	0.27
CESM1-BGC	407	697	1121	1.92	4.80	7.34	1.12	2.85	4.64	0.18	0.48	0.61
FGOALS-s2.0	404	636	993	1.89	4.31	6.70	1.09	2.57	4.23	0.15	0.20	0.20
GFDL-ESM2G	395	616	967	1.77	4.14	6.56	1.04	2.49	4.12	0.10	0.12	0.09
GFDL-ESM2M	400	621	964	1.83	4.18	6.54	1.09	2.52	4.13	0.15	0.15	0.10
HadGEM2-ES	411	636	983	1.98	4.31	6.64	1.18	2.60	4.20	0.24	0.23	0.17
INM-CM4	386	591	897	1.64	3.92	6.15	0.92	2.36	3.86	−0.02	−0.01	−0.17
IPSL-CM5A-LR	375	573	908	1.48	3.75	6.22	0.86	2.21	3.87	−0.08	−0.16	−0.16
MIROC-ESM	398	658	1121	1.81	4.50	7.35	1.06	2.67	4.58	0.12	0.30	0.55
MPI-ESM-LR r1	383	590	948	1.60	3.91	6.45	0.95	2.31	4.03	0.01	−0.06	0.00
MRI-ESM1	361	516	778	1.28	3.20	5.39	0.74	1.89	3.33	−0.20	−0.48	−0.70
NorESM1-ME	391	667	1070	1.72	4.57	7.09	0.98	2.68	4.46	0.04	0.31	0.43
Multi-model Mean	392	621	980	1.72	4.18	6.63	1.00	2.48	4.17	0.06	0.11	0.14
CCTM Estimate	385	600	948	1.62	4.01	6.45	0.94	2.37	4.03	—	—	—
Historical + RCP 8.5	385	590	917	1.63	3.91	6.27	0.94	2.32	3.93	0.00	−0.05	−0.10

References

R. J. Andres, J. S. Gregg, L. Losey, G. Marland, and T. A. Boden. Monthly, global emissions of carbon dioxide from fossil fuel consumption. *Tellus B*, 63(3):309–327, July 2011. doi: 10.1111/j.1600-0889.2011.00530.x.

R. J. Andres, T. A. Boden, F.-M. Bréon, P. Ciais, S. Davis, D. Erickson, J. S. Gregg, A. Jacobson, G. Marland, J. Miller, T. Oda, J. G. J. Olivier, M. R. Raupach, P. Rayner, and K. Treanton. A synthesis of carbon dioxide emissions from fossil-fuel combustion. *Biogeosci.*, 9(5):1845–1871, May 2012. doi: 10.5194/bg-9-1845-2012.

P. M. Cox, D. Pearson, B. B. Booth, P. Friedlingstein, C. Huntingford, C. D. Jones, and C. M. Luke. Sensitivity of tropical carbon to climate change constrained by carbon dioxide variability. *Nature*, 494(7437):341–344, Feb. 2013. doi: 10.1038/nature11882.

A. Hall and X. Qu. Using the current seasonal cycle to constrain snow albedo feedback in future climate change. *Geophys. Res. Lett.*, 33(3):L03502, Feb. 2006. doi: 10.1029/2005GL025127.

S. Khatiwala, T. Tanhua, S. Mikaloff Fletcher, M. Gerber, S. C. Doney, H. D. Graven, N. Gruber, G. A. McKinley, A. Murata, A. F. Ríos, and C. L. Sabine. Global ocean storage of anthropogenic carbon. *Biogeosci.*, 10(4): 2169–2191, Apr. 2013. doi: 10.5194/bg-10-2169-2013.

M. Meinshausen, S. Smith, K. Calvin, J. Daniel, M. Kainuma, J.-F. Lamarque, K. Matsumoto, S. Montzka, S. Raper, K. Riahi, A. Thomson, G. Velders, and D. P. van Vuuren. The RCP greenhouse gas concentrations and their extensions from 1765 to 2300. *Clim. Change*, 109(1):213–241, Nov. 2011. doi: 10.1007/s10584-011-0156-z.

C. L. Sabine, R. A. Feely, N. Gruber, R. M. Key, K. Lee, J. L. Bullister, R. Wanninkhof, C. S. Wong, D. W. R. Wallace, B. Tilbrook, F. J. Millero, T.-H. Peng, A. Kozyr, T. Ono, and A. F. Rios. The oceanic sink for anthropogenic CO_2. *Science*, 305(5682):367–371, July 2004. doi: 10.1126/science.1097403.